Kinetic and Catalytic Aspects in Melt Transesterification of Dimethyl Terephthalate With Ethylene Glycol

E. SANTACESARIA,[1]* F. TRULLI,[1] L. MINERVINI,[1] M. DI SERIO,[2] R. TESSER,[3] and S. CONTESSA[3]

[1]Dipartimento di Chimica dell'Università, Via Mezzocannone 4 (80130) Napoli, Italy; [2]Dipartimento di Fisica dell'Università di Salerno, Baronissi, Salerno, Italy; [3]Montefibre S.p.A., Acerra, Napoli, Italy

SYNOPSIS

The kinetics of melt transesterification of dimethyl terephthalate with ethylene glycol in the presence of zinc acetate as catalyst has been studied in semibatch conditions. We observed that this reaction occurs with the formation of many oligomers characterized from the terminal groups of the chains that can be hydroxyl–hydroxyl, methyl–hydroxyl or methyl–methyl. Experimental runs have been performed at different temperatures, initial reagents ratios, and catalyst concentrations, following the amount of methanol released during the time as well as the concentration of any kind of oligomer. All the oligomers have been identified and determined by HPLC analysis. A classic kinetic model based on a complex reaction scheme containing four or five reaction sequences has been developed.

The scheme with four sequences foresees 24 oligomeric species involved in 58 different reactions, while the scheme with five sequences has 48 oligomeric species involved in 228 reactions. Despite the large number of oligomers and occurring reactions, only two kinetic parameters and two equilibrium constants are necessary to simulate the kinetic behaviour of all the oligomers. A kinetic constant is related to the reaction of a methyl group with a hydroxyl of ethylene glycol, while the other corresponds to the reaction of a methyl group with a hydroxyl in a chain. Both kinetic constants show an activation energy of about 15 kcal/mol. We observed a nonlinear correlation between activity and catalyst concentration and interpreted this fact by assuming two different catalytic activity levels for a dissociated and an undissociated zinc ionic couple, respectively.

INTRODUCTION

The melt transesterification of dimethyl terephthalate (DMT) with ethylene glycol (EG) is performed in industry as the first stage for the production of polyethylene terephthalate (PET). The reaction is promoted by catalysts such as zinc, manganese, lead acetates, and many others, used alone or in mixtures. Many papers[1–5] appeared in literature to compare the activities of several catalysts. Catalysts activities were usually evaluated by measuring the amounts of methanol released with time, as a consequence of the reaction. It was a general opinion that by operating with a ratio EG/DMT = 2, bishydroxyethyl terephthalate (BHET) is formed as the main reaction product. For this reason, in many articles[1,6–7] dealing with the kinetics of polycondensation that is the second stage of the PET synthesis, BHET is usually assumed as the reaction monomer.

Besnoin et al.[1,6–8] have recently shown by HPLC analysis that in the melt transesterification of DMT with EG, substantial amounts of many compounds with different molecular weight are formed together with BHET. Three types of compounds have been recognized differing for the two terminal groups, i.e., hydroxyl–hydroxyl, methyl–hydroxyl, methyl–methyl, respectively. Besnoin et al.[1,6] suggested a kinetic model to simulate the evolution with time of all the possible oligomers and of the methanol release. They determined the kinetic parameters on the basis of the collected experimental data, that is,

* To whom correspondence should be addressed.

Journal of Applied Polymer Science, Vol. 54, 1371–1384 (1994)
 CCC 0021-8995/94/091371-14

the distributions of all the oligomers except for those with methyl–methyl terminal groups that were not separated in the HPLC analysis.

This approach represents a remarkable improvement compared to the past, and is worth being deepened, considering that oligomers with methyl–methyl or methyl–hydroxyl terminal groups will presumably behave very differently in the subsequent stage of polycondensation to PET from those with hydroxyl–hydroxyl terminal groups. Moreover, the assumption formulated in the past that the mixtures of the described oligomers can be considered as pure BHET is wrong and may provide erroneous information about the characteristics of the final product PET, because the average molecular weight of the polymer, in this case, is calculated on the basis of a unique distribution instead of three that can be forecast when the mentioned oligomers are considered as starting reagents.

In the present work, we have first of all improved the HPLC analytical method compared to that described by Besnoin et al.[1,6] With our method, all the possible oligomers have been separated, identified, and determined quantitatively. Then, a different kinetic approach has been developed based on the classic definition of the complex reaction scheme characterized by combinations of many simultaneous and consecutive reactions. From this scheme, the existence of different reaction sequences can be observed. The products obtained in a reaction sequence are the reactants for the next one.

At any subsequent reaction sequence, reactants, products, and reactions involving them strongly increase. We have, for example, two reactant species in the first sequence, i.e., EG and DMT, and one reaction giving methyl hydroxyethylterepthalate (MHET) as product, together with methanol. In the second sequence, we have three reactants, three products, plus methanol, all involved in three reactions. We have developed this reaction scheme until the fifth stage, corresponding to 48 different oligomeric species involved in 228 different reactions. However, we observed that both the kinetic runs performed by us and by Besnoin et al.[1,6] can be interpreted giving exactly the same results also by truncating the reaction scheme at the fourth stage corresponding to 24 oligomeric species involved in 58 different reactions. The reactions in this scheme are different because they occur between different oligomeric species but are obviously of the same type, that is, a hydroxyl group reacts with a methyl group to give condensation and methanol release. The unique difference, in agreement with previous literature,[1,6,7] is the different reactivity of the hydroxyls on the terminal groups of the oligomeric chains, and those on free EG. Reactivities seem to be poorly affected by the length of the chains. Therefore, notwithstanding, the complexity of the kinetic model for a given type and amount of catalyst and at a fixed temperature only two kinetic parameters and two equilibrium constants are necessary to completely describe the evolution with time of all the possible oligomeric species and of the amount of methanol released. In particular, in the case of a zinc acetate catalyst, in a moderate concentration, only one kinetic parameter is necessary because the reactivity of EG hydroxyls resulted about 1.6 times greater that of the hydroxyls on the oligomeric chains, independently of temperature. In fact, activation energies resulted quite similar for both reactions and the difference in reactivity must be ascribed to the preexponential factors, only.

The described kinetic model has been applied for the interpretation of the kinetic runs performed at different EG/DMT ratios, temperatures, and catalyst concentrations. The kinetic parametes of the model have been determined by mathematical regression analysis on the experimental data.

When the reaction is performed at very low zinc acetate concentrations, the reactivities of EG hydroxyls strongly increase compared to those of the hydroxyls on the oligomer chains remainig constant.

A discussion about these features and the reaction mechanism will conclude the article.

EXPERIMENTAL SECTION

Development of the Kinetic Model on the Basis of the Reaction Scheme

As mentioned in the previous section, three types of oligomers can be formed as a consequence of the transesterification reactions, differing for the terminal groups. We indicate the three different types of oligomers obtained by adopting the following general formulas:

$$X_n = H_3C-[OOC-\phi-COOC_2H_4]_n -OOC-\phi-COOCH_3 \quad n = 0, n$$

$$Y_n = HOC_2H_4-[OOC-\phi-COOC_2H_4]_n-OH \quad n = 0, n$$

$$Z_n = HOC_2H_4-[OOC-\phi-COOC_2H_4]_{n-1} -OOC-\phi-COOCH_3 \quad n = 1, n$$

Therefore, X_0 corresponds to DMT, Y_0 to EG, Z_1 to MHET, Y_1 to BHET, etc. Adopting this ab-

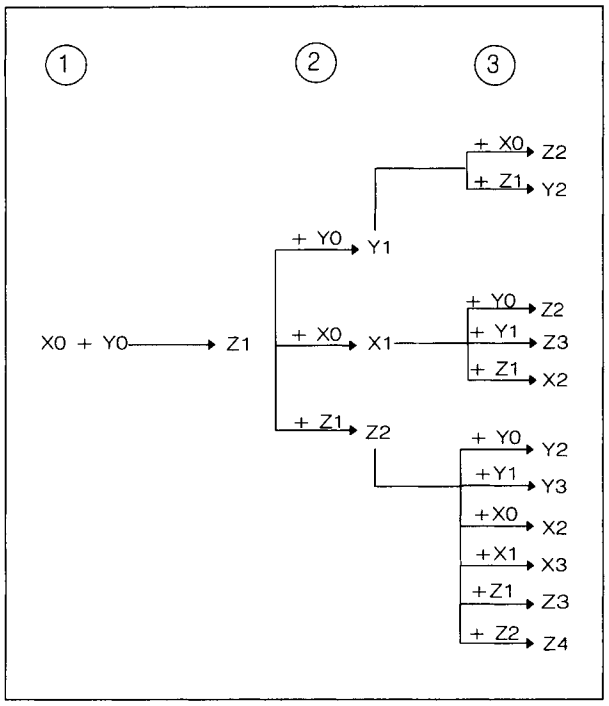

Figure 1 Reaction scheme truncated at the third sequence or stage.

breviated form to represent the different oligomers, it is easy to draw a reaction scheme as that reported in Figure 1. This reaction scheme, given as an example, is truncated at the third stage of sequence of reactions, while in Table I all the reactions are reported in detail, occurring in correspondence with any single sequence until the fourth one, that is, 58 different reactions are shown involving 24 different oligomers. We have developed also the fifth sequence in a similar way, reaching a total of 228 reactions involving 48 different oligomers we do not report here for reason of briefness.

Observing the scheme of Figure 1 and the list of reactions of Table I, some oligomers are involved in many reactions; therefore, in order to follow the evolution of these oligomers with time, it is useful to make the stoichiometric matrix α_{ij} and define the rate of formation of the i species as:

$$r_i = \sum_{j=1}^{m} \alpha_{ij} r_j \qquad (1)$$

by truncating the reaction sequences at the fourth, $m = 58$ and $i = 1,24$. Table II reports the rates of formation or disappearing of the 24 oligomeric species of Table I obtained by properly applying relation (1). It is now necessary to furnish the kinetic expressions for all the r_j with $j = 1,58$. Assuming, as a first approximation, that reactivity is not affected by the chain length, in Table I it is possible to recognize six different types of reactions, i.e., those reported in Table III. It is reasonable to assume that chains containing different terminal groups are less reactive by a factor of 1/2 than those having terminal groups of the same type.

By assuming a second-order kinetic law, the six equations r_{A-F} still reported in Table III are obtained. As it can be seen, only two kinetic constants, k_1 and k_2, and two corresponding equilibrium constants, K_{eq1} and K_{eq2}, appear in the above-mentioned kinetic equations. The kinetic constant k_1 is related to the reaction of a methyl group with the hydroxyl of free EG, while k_2 is related to the reaction of a methyl group with a hydroxyl of an oligomeric chain.

By substituting in Table II r_j, where $j = 1,58$, with the proper expressions of r_A, r_B, r_C, r_D, r_E, and r_F, the resulting 25 differential equations can be integrated numerically giving the evolution with time of the amounts of all the oligomeric species and of the released methanol. The methanol partition between the liquid and vapor phase has been considered to have an ideal behavior and the methanol concentration has been calculated by the Raoult law, i.e.,

$$X_M = Y_M P/P^0 \cong 1/P^0 \qquad (2)$$

where, for methanol:

$$P^0 = \exp[18.5878 - 3626.55/(T - 34.29)]/760 \qquad (3)$$

Methods, Techniques, and Reagents

Kinetic runs have been carried out in a 500 mL jacketed glass reactor, fitted both with a three-necked reactor head and with a distillation system as schematized in Figure 2. The reactor is kept isothermal by stirring and by recirculating a thermostated fluid in the jacket. As the polycondensation reactions are all equilibrium reactions, the formed methanol must be removed as soon as possible. It was conveyed to a jacketed column, packed with Raschig rings, kept at 100°C with a recirculating thermostated fluid, then led to a Liebig condenser and finally to a graduate receiver. The head of the reactor was heated and insulated in order to avoid methanol vapors condensation. In this way, methanol is efficiently removed from the reactor and completely collected while EG is totally refluxed. The reactor was stirred with a magnetic bar rotating at about 700–1000 rpm.

Table I List of the Reactions Occurring in a Scheme Considering Four Sequences

1 Stage

1) $X_0 + Y_0 \Leftrightarrow Z_1 + CH_3OH$

2 Stage

2) $Z_1 + Y_0 \Leftrightarrow Y_1 + CH_3OH$
3) $Z_1 + X_0 \Leftrightarrow X_1 + CH_3OH$
4) $Z_1 + Z_1 \Leftrightarrow Z_2 + CH_3OH$

3 Stage

5) $Z_2 + Y_0 \Leftrightarrow Y_2 + CH_3OH$
6) $Z_2 + Y_1 \Leftrightarrow Y_3 + CH_3OH$
7) $Z_2 + X_0 \Leftrightarrow X_2 + CH_3OH$
8) $Z_2 + X_1 \Leftrightarrow X_3 + CH_3OH$
9) $Z_2 + Z_1 \Leftrightarrow Z_3 + CH_3OH$
10) $Z_2 + Z_2 \Leftrightarrow Z_4 + CH_3OH$
11) $X_1 + Y_0 \Leftrightarrow Z_2 + CH_3OH$
12) $X_1 + Y_1 \Leftrightarrow Z_3 + CH_3OH$
13) $X_1 + Z_1 \Leftrightarrow X_2 + CH_3OH$
14) $Y_1 + X_0 \Leftrightarrow X_2 + CH_3OH$
15) $Y_1 + X_1 \Leftrightarrow Y_2 + CH_3OH$

4 Stage

16) $Z_4 + Y_0 \Leftrightarrow Y_4 + CH_3OH$
17) $Z_4 + Y_1 \Leftrightarrow Y_5 + CH_3OH$
18) $Z_4 + Y_2 \Leftrightarrow Y_6 + CH_3OH$
19) $Z_4 + Y_3 \Leftrightarrow Y_7 + CH_3OH$
20) $Z_4 + X_0 \Leftrightarrow X_4 + CH_3OH$
21) $Z_4 + X_1 \Leftrightarrow X_5 + CH_3OH$
22) $Z_4 + X_2 \Leftrightarrow X_6 + CH_3OH$
23) $Z_4 + X_3 \Leftrightarrow X_7 + CH_3OH$
24) $Z_4 + Z_1 \Leftrightarrow Z_5 + CH_3OH$
25) $Z_4 + Z_2 \Leftrightarrow Z_6 + CH_3OH$
26) $Z_4 + Z_3 \Leftrightarrow Z_7 + CH_3OH$
27) $Z_4 + Z_4 \Leftrightarrow Z_8 + CH_3OH$
28) $Z_3 + Y_0 \Leftrightarrow Y_3 + CH_3OH$
29) $Z_3 + Y_1 \Leftrightarrow Y_4 + CH_3OH$
30) $Z_3 + Y_2 \Leftrightarrow Y_5 + CH_3OH$
31) $Z_3 + Y_3 \Leftrightarrow Y_6 + CH_3OH$
32) $Z_3 + X_0 \Leftrightarrow X_3 + CH_3OH$
33) $Z_3 + X_1 \Leftrightarrow X_4 + CH_3OH$
34) $Z_3 + X_2 \Leftrightarrow X_5 + CH_3OH$
35) $Z_3 + X_3 \Leftrightarrow X_6 + CH_3OH$
36) $Z_3 + Z_1 \Leftrightarrow Z_4 + CH_3OH$
37) $Z_3 + Z_2 \Leftrightarrow Z_5 + CH_3OH$
38) $Z_3 + Z_3 \Leftrightarrow Z_6 + CH_3OH$
39) $Z_3 + Y_0 \Leftrightarrow Z_4 + CH_3OH$
40) $Z_3 + Y_1 \Leftrightarrow Z_5 + CH_3OH$
41) $X_3 + Y_2 \Leftrightarrow Z_6 + CH_3OH$
42) $X_3 + Y_3 \Leftrightarrow Z_7 + CH_3OH$
43) $X_3 + Z_1 \Leftrightarrow X_4 + CH_3OH$
44) $X_3 + Z_2 \Leftrightarrow X_5 + CH_3OH$
45) $X_2 + Y_0 \Leftrightarrow Z_4 + CH_3OH$
46) $X_2 + Y_1 \Leftrightarrow Z_4 + CH_3OH$
47) $X_2 + Y_2 \Leftrightarrow Z_5 + CH_3OH$
48) $X_2 + Y_3 \Leftrightarrow Z_6 + CH_3OH$
49) $X_2 + Z_1 \Leftrightarrow X_3 + CH_3OH$
50) $X_2 + Z_2 \Leftrightarrow X_4 + CH_3OH$
51) $Y_3 + X_0 \Leftrightarrow Z_4 + CH_3OH$
52) $Y_3 + X_1 \Leftrightarrow Z_5 + CH_3OH$
53) $Y_3 + Z_1 \Leftrightarrow Y_4 + CH_3OH$
54) $Y_3 + Z_2 \Leftrightarrow Y_5 + CH_3OH$
55) $Y_2 + X_0 \Leftrightarrow Z_3 + CH_3OH$
56) $Y_2 + X_1 \Leftrightarrow Z_4 + CH_3OH$
57) $Y_2 + Z_1 \Leftrightarrow Y_3 + CH_3OH$
58) $Y_2 + Z_2 \Leftrightarrow Y_4 + CH_3OH$

Normally, 100 g of DMT was put in the reactor, and heated at the reaction temperature, which is higher than the DMT melting temperature, 140°C; then an appropriate amount of EG was added according to the desired EG/DMT ratio. At last, the catalyst zinc acetate ($Zn(Ac)_2 \cdot 2H_2O$) previously dissolved in about 15 mL of EG was added. The time when the first drop of methanol appeared in the condenser was considered as the beginning of the reaction. Samples of the reaction mixture were withdrawn at different reaction times and submitted to HPLC analysis. At the corresponding times, the amount of collected methanol was carefully read.

Kinetic runs were performed at different EG/DMT ratios, different temperatures, and different catalyst concentrations by measuring during the time both the methanol released and the evolution of all the oligomers produced. A list of some of the kinetic runs performed is reported in Table IV, together with the operative conditions applied.

The HPLC analysis of the samples withdrawn during the kinetic runs were carried out with a JASCO/PU 980 apparatus using a Spherisorb S5W column of Labservice Analytica, that is, a stainless steel column with 25 cm length and 0.46 cm diameter filled with 5 μm silica particles. The samples were

Table II Rates of Formation or Disappearing of All the Oligomer Species Appearing in Table I

$$r_{X0} = r_{DMT} = -r_1 - r_3 - r_7 - r_{14} - r_{20} - r_{32} - r_{51} - r_{55} = -r_A - 3r_C - 4r_D$$
$$r_{X1} = r_3 - r_8 - r_{11} - r_{12} - r_{13} - r_{21} - r_{33} - r_{52} - r_{56} = -r_A - 3r_C - 5r_D$$
$$r_{X2} = r_7 + r_{13} - r_{22} - r_{34} - r_{45} - r_{46} - r_{47} - r_{48} - r_{49} - r_{50} = -r_A - 3r_C - 2r_D$$
$$r_{X3} = r_8 - r_{23} + r_{32} - r_{35} - r_{39} - r_{40} - r_{41} - r_{42} - r_{43} - r_{44} + r_{49} = -r_A - 3r_C - r_D$$
$$r_{X4} = r_{20} + r_{33} + r_{43} + r_{50} = 4r_D$$
$$r_{X5} = r_{21} + r_{34} + r_{44} = 3r_D$$
$$r_{X6} = r_{22} + r_{35} = 2r_D$$
$$r_{X7} = r_{23} = r_D$$

$$r_{Y0} = r_{EG} = -r_1 - r_2 - r_5 - r_{11} - r_{16} - r_{28} - r_{39} - r_{45} = -4r_A - 4r_B$$
$$r_{Y1} = r_{BHET} = r_2 - r_6 - r_{12} - r_{14} - r_{15} - r_{17} - r_{29} - r_{40} - r_{46} = r_B - 5r_C - 3r_F$$
$$r_{Y2} = r_5 + r_{15} - r_{18} - r_{30} - r_{41} - r_{47} - r_{55} - r_{56} - r_{57} - r_{58} = r_B - 3r_C - 4r_F$$
$$r_{Y3} = r_6 - r_{19} + r_{28} - r_{31} - r_{42} - r_{48} - r_{51} - r_{52} - r_{53} - r_{54} + r_{57} = r_B - 4r_C - 2r_F$$
$$r_{Y4} = r_{16} + r_{29} + r_{53} + r_{58} = r_B + 3r_F$$
$$r_{Y5} = r_{17} + r_{30} + r_{54} = 3r_F$$
$$r_{Y6} = r_{18} + r_{31} = 2r_F$$
$$r_{Y7} = r_{19} = r_F$$

$$r_{Z1} = r_{MHET} = r_1 - r_2 - r_3 - 2r_4 - r_9 - r_{13} - r_{15} - r_{24} - r_{36} - r_{43} - r_{49} - r_{53} - r_{57} = r_A - r_B - r_C - 2r_D - 5r_E - 2r_F$$
$$r_{Z2} = r_4 - r_5 - r_6 - r_7 - r_8 - r_9 - 2r_{10} + r_{11} + r_{14} - r_{25} - r_{37} - r_{44} - r_{50} - r_{54} - r_{58} = r_A - r_B + r_C - 4r_D - 4r_E - 3r_F$$
$$r_{Z3} = r_9 + r_{12} - r_{26} - r_{28} - r_{29} - r_{30} - r_{31} - r_{32} - r_{33} - r_{34} - r_{34} - r_{35} - r_{36} - r_{37} - 2r_{38} + r_{45} + r_{55}$$
$$= r_A - r_B + 2r_C - 4r_D - 4r_E - 3r_F$$
$$r_{Z4} = r_{10} - r_{16} - r_{17} - r_{18} - r_{19} - r_{20} - r_{21} - r_{22} - r_{23} - r_{24} - r_{25} - r_{26} - 2r_{27} + r_{36} + r_{39} + r_{46} + r_{51} + r_{56}$$
$$= r_A - r_B + 3r_C - 4r_D - 3r_E - 3r_F$$
$$r_{Z5} = r_{24} + r_{37} + r_{40} + r_{47} + r_{52} = 3r_C + 2r_E$$
$$r_{Z6} = r_{25} + r_{38} + r_{41} + r_{48} = 2r_C + 2r_E$$
$$r_{Z7} = r_{26} + r_{42} = r_C + r_E$$
$$r_{Z8} = r_{27} = r_E$$

prepared for the analysis by dissolving about 2 mg of the reaction mixture in 10 cm^3 of a solvent containing 98% by volume of chloroform and 2% of 1,1,1–3,3,3 Hexafluor-2-propanol. The mobile phase fed to the colum with feed rate 1 mL/min, was a mixture of hexane (A) and dioxane (B), with the composition changing with time as reported in Table V. UV detector JASCO 975 operating at 254 nm was used. In Figure 3, a chromatogram is reported as an

Table III Kinetic Equations Applied to the Model

Types of reactions

A) $X_i + Y_0 \Leftrightarrow Z_{i+1} + CH_3OH$	K_{eq1}	K_1
B) $Z_i + Y_0 \Leftrightarrow Y_i + CH_3OH$	K_{eq1}	$K_1/2$
C) $X_i + Y_i \Leftrightarrow Z_{2i+1} + CH_3OH$	K_{eq2}	K_2
D) $X_i + Z_i \Leftrightarrow X_{i+1} + CH_3OH$	K_{eq2}	$K_2/2$
E) $Z_i + Z_i \Leftrightarrow Z_{2i} + CH_3OH$	K_{eq2}	$K_2/2$
F) $Z_i + Y_i \Leftrightarrow Y_{2i} + CH_3OH$	K_{eq2}	$K_2/2$

Corresponding kinetic equations

$$r_A = K_1^*[X_i]^*[Y_0] - (K_1/K_{eq})^*[Z_{i+1}]^*[CH_3OH]$$
$$r_B = (K_1/2)^*[Z_i]^*[Y_0] - (K_1/2K_{eq1})^*[Y_i]^*[CH_3OH]$$
$$r_C = K_2^*[X_i]^*[Y_i] - (K_2/K_{eq2})^*[Z_{2i+1}]^*[CH_3OH]$$
$$r_D = (K_2/2)^*[X_i]^*[Z_i] - (K_2/2K_{eq2})^*[X_{i+1}]^*[CH_3OH]$$
$$r_E = (K_2/2)^*[Z_i]^*[Z_i] - (K_2/2K_{eq2})^*[Z_{2i}]^*[CH_3OH]$$
$$r_F = (K_2/2)^*[Z_i][Y_i] - (K_2/2K_{eq2})^*[Y_{2i}]^*[CH_3OH]$$

Table IV List of the Kinetic Runs Performed and Corresponding Operative Conditions

Runs	DMT (g)	EG/DMT Molar Ratio	$[Zn(Ac)_2]$ mol/L	Temperature °C
1	95.0	2	3.60 E-3	160
2	97.0	2	3.60 E-3	165
3	95.1	2	3.60 E-3	170
4	97.9	2	9.28 E-3	180
5	97.4	2	6.57 E-3	180
6	96.2	2	3.70 E-3	183
7	98.1	2	1.87 E-3	180
8	96.5	2	9.18 E-4	180
9	94.1	2	5.75 E-4	180
10	92.4	2	3.62 E-4	180
11	96.0	3	3.70 E-3	180
12	99.2	1	4.71 E-3	180

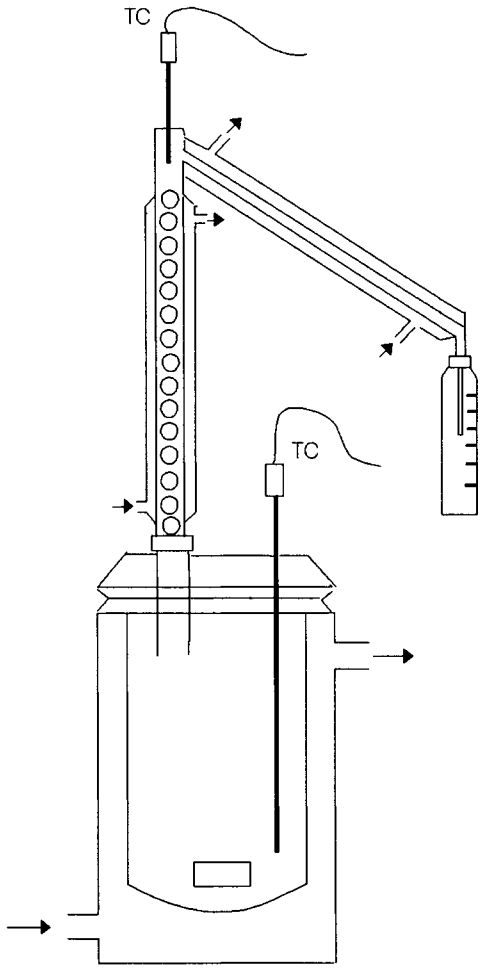

Figure 2 Scheme of the apparatus used for the kinetic runs.

example of the obtainable separations. As it can be seen, the different species are eluated on the basis of their different polarities and, for the same polarity, on the basis of their different molecular weights. Therefore, it is possible to very satisfactorily separate all the oligomers. For the quantitative determination of the different oligomers, DMT has been

Table V Elution Gradient Used in the HPLC Analysis

Time (Minutes)	*n*-Hexane % Volume	1,4-Dioxane % Volume
0.0	60	40
2.0	60	40
5.5	55	45
11.0	52	48
15.0	52	48
22.0	45	55

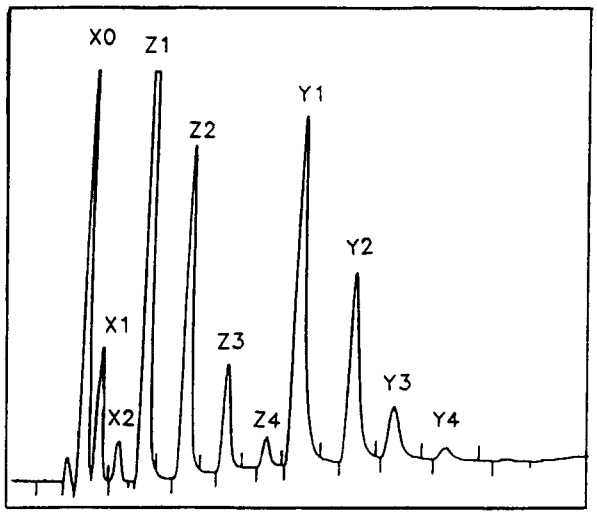

Figure 3 Example of a chromatogram obtained with the HPLC analysis.

assumed as reference substance; then, the response factors have been estimated for all the oligomers assuming the same contribution for each aromatic ring in the molecule.

The HPLC method described must be considered an improvement of the method suggested by Besnoin et al.[1,6] which was developed from a method suggested by L. M. Zaborsky.[9]

The reagents employed, DMT, EG, and zinc acetate have been furnished at the highest purity available from Aldrich Co.

RESULTS

As shown in Table IV, kinetic runs have been performed at three different EG/DMT ratios corresponding to the values 1, 2, and 3. Then, runs at different temperatures and catalyst concentrations have been carried out by taking the EG/DMT ratio constant and equal to 2. The amount of methanol released during the reaction has been experimentally determined in two different ways, that is, directly, through the measurement of the volume of the methanol recovered in the condenser, and indirectly from the mass balance performed on the residual methyl groups in the reaction mixture, as resulting from the HPLC analysis of all the oligomers, compared with the methyl groups contained in the initial amount of DMT. Therefore, we can define the yields of methanol in the following two ways:

$$\eta = \frac{n_{CH_3OH}}{2n^0_{DMT}} = \frac{2n^0_{DMT} - 2\sum_{i=0}^{n} n_{x_n} - \sum_{i=1}^{n} n_{Z_n}}{2n^0_{DMT}} \quad (4)$$

Table VI Optimized Kinetic and Equilibrium Parameter Obtained from the Mathematical Regression Analysis Performed on the Single Runs Listed in Table IV

Runs	K_1 (L^2 mol^{-2} $Minutes^{-1}$)	K_2 (L^2 mol^{-2} $Minutes^{-1}$)	K_{eq1}	K_{eq2}
1	1.75	1.46	0.264	0.234
2	2.67	1.65	0.234	0.202
3	3.67	272	0.210	0.181
4	2.63	2.73	0.166	0.184
5	4.19	2.51	0.460	0.170
6	6.05	3.67	0.152	0.135
7	5.45	4.13	0.161	0.198
8	6.62	3.47	0.162	0.474
9	11.52	2.38	0.380	1.173
10	17.90	3.07	0.225	0.209
11	4.0	2.89	0.313	0.227
12	4.85	4.44	0.072	0.154

The correspondence of the yields calculated in the two ways shown in Eq. (4) is a guaranty for the reliability of the data collected.

The evolution with time of DMT and of all the oligomers formed in the reaction has been plotted after HPLC analysis of the samples withdrawn at different times.

Kinetic data collected for each run have been arranged in four types of plots, one giving methanol yields as a function of time, the other three giving the evolution with time of the oligomers of the type X, Y, and Z, respectively. All these kinetic data collected for each run have been submitted to mathematical regression analysis[10] by applying the described kinetic model and looking for the minimum of the following objective function:

$$\Phi(\beta) = \left(\frac{\eta_s - \eta_c}{\eta_s}\right)^2 + \sum_i \left(\frac{[X_{is}] - [X_{ic}]}{[X_{is}]}\right)^2 + \sum_i \left(\frac{[Y_{is}] - [Y_{ic}]}{[Y_{is}]}\right)^2 + \sum_i \left(\frac{[Z_{is}] - [Z_{ic}]}{[Z_{is}]}\right)^2 \quad (5)$$

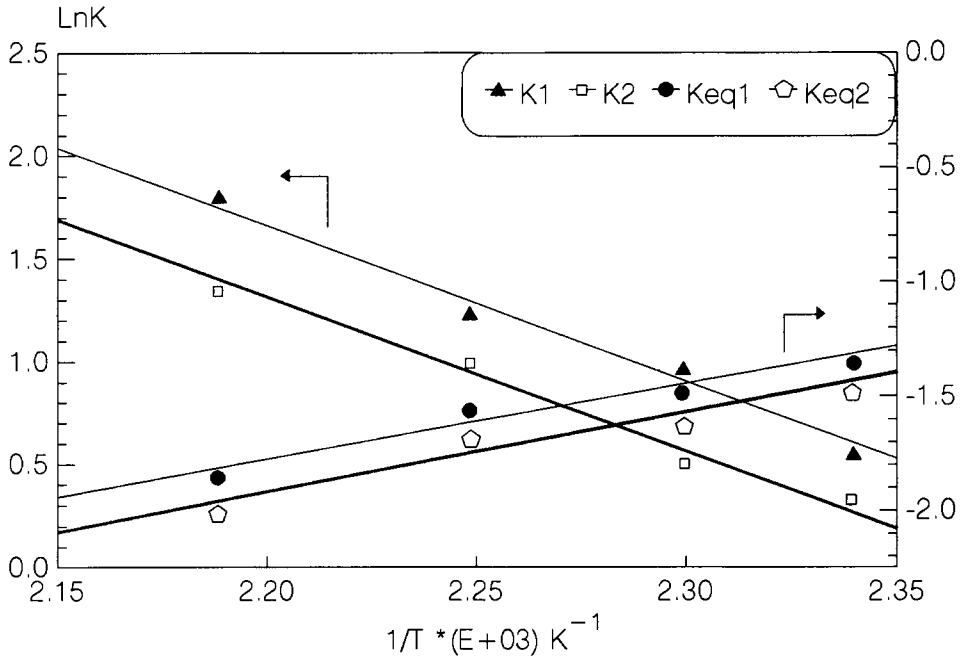

Figure 4 Arrhenius–Van't Hoff-type plot obtained for the kinetic and the equilibrium constants, respectively (runs 1, 2, 3, and 6).

Table VII Activation Energies, Enthalpy Changes, and Preexponential Factors Obtained from the Runs Performed at Different Temperatures

	Preexponential Factors	Activation Energies or Enthalpy Changes (cal/mol)
K_1 (L^2 mol^{-2} $minutes^{-1}$)	(8.6 ± 0.5)*E + 7	15002 ± 750
K_2 (L^2 mol^{-2} $minutes^{-1}$)	(5.2 ± 0.6)*E + 7	14863 ± 743
K_{eq1}	(1.1 ± 0.8)*E − 4	−6597 ± 264
K_{eq2}	(8.4 ± 0.7)*E − 6	−8802 ± 352

where the subscript s corresponds to experimental, while c to calculated.

The final result of this statistical regression is summarized in Table VI where the optimal kinetic and equilibrium parameters obtained for each run of Table IV are reported.

The first observation is that the variation of the EG/DMT ratio (see runs 7, 11, and 12) does not produce significant variations in the kinetic parameters. This means that the second-order kinetic laws adopted and the other assumptions introduced are reliable. The second observation is that temperature and catalyst concentration affect the kinetic parameters. By arranging in Figure 4 the kinetic and equilibrium parameters obtained at different temperatures, for the runs 1, 2, 3, and 6 in an Arrhenius-Van't Hoff-type plot, straight lines are obtained, the slopes of which, respectively, give the activation energies and the enthalpy changes. The obtained values of these parameters, tested on many other runs than those of Table IV, are reported together with the corresponding preexponential factor in Table VII. It is interesting to observe that the activation energies for k_1 and k_2 are quite similar, that is, the difference in the reactivity of a methyl group with an EG hydroxyl or of an oligomer chain is mainly due to the difference of the preexponential factor. It is of practical interest to assume for k_1 and k_2 exactly the same average activation energy of 14932 cal/mol and correct the corresponding preexponential factors. We obtain in this case:

$$k_1 = 8.71 \times 10^7 \exp(-14932/RT)$$

$$k_2 = k_1/1.6 \qquad (6)$$

So, we have the advantage of being able to simulate melt transesterification with a reduced number of parameters without loosing in accuracy. The value

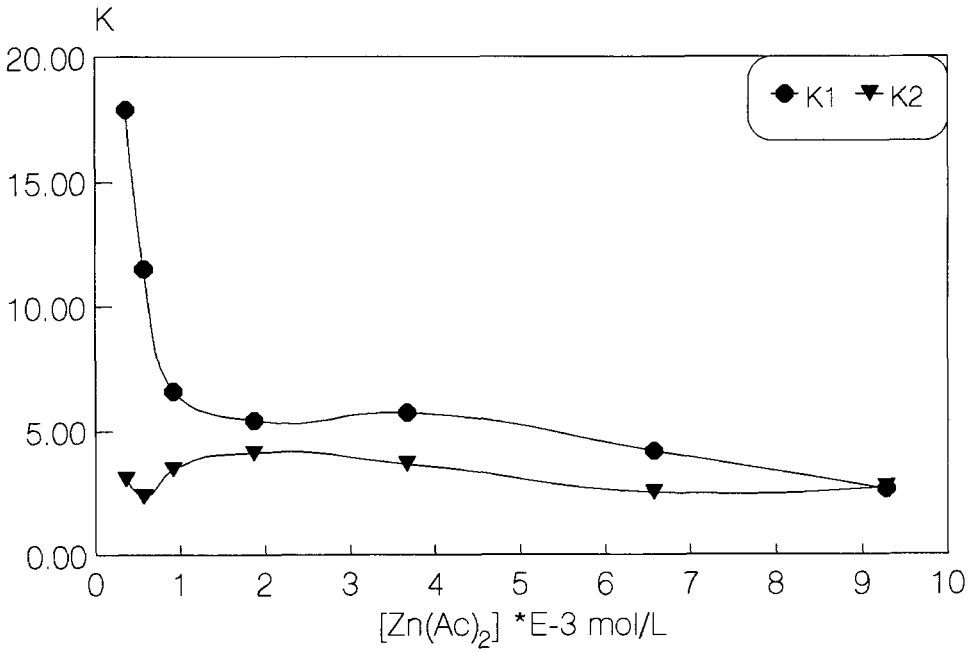

Figure 5 Effect of the catalyst concentration on the kinetic constants k_1 and k_2 (runs 4–10). Data of run 6 have been normalized at 180°C.

obtained for activation energies is in good agreement with some values reported by the literature.[3,11,15]

The ratio $k_1/k_2 = 1.6$ is fairly in agreement with the value found by other authors.[1,7]

The effect of the catalyst concentration on the kinetic parameters is reported in Figure 5 (runs 4–10). Data of run 6 have been normalized at 180°C. It is interesting to observe a small influence on both k_1 and k_2 for high catalyst concentrations; however, when the catalyst concentration decreases, k_1 strongly increases, while k_2 remains nearly unchanged. That is, zinc acetate at low concentrations shows high selectivity in promoting the reaction of methyl groups with free EG. This fact could be of practical interest and give useful insights on the reaction mechanism.

At last, examples of the simulations obtained with the described kinetic model are reported in Figures 6–12. Figure 6 reports methanol yields obtained at different times in the runs 1, 3, and 6 of Table IV, performed at different temperatures. An example of the agreement obtained in the distribution of the oligomers is reported in Figure 7 corresponding to run 6 of Table IV performed at 183°C. In Figure 8, methanol yields for different EG/DMT ratios, corresponding to run 6, 11, and 12 of Table IV are reported, while in Figure 9, the agreement obtained in the oligomers distribution related to run 11, is shown as an example. Finally, methanol yields for the runs performed at different catalyst concentrations, that is, runs 5, 6, and 7 of Table IV, are reported in Figure 10, while in Figure 11 a comparison is reported, as an example, of the difference obtained in methanol yields determined, respectively, from direct observation and from HPLC analysis related to run 6. In Figure 12, the evolution with time of the oligomers in the runs performed at the lowest (run 10 of Table IV) and at the highest (run 4 of Table IV) catalyst concentration, respectively, are

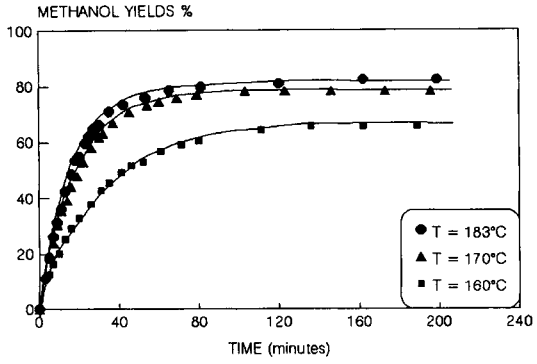

Figure 6 Methanol yields at different times for runs performed at different temperatures (runs 1–3–6). Symbols are experimental data, lines are calculated.

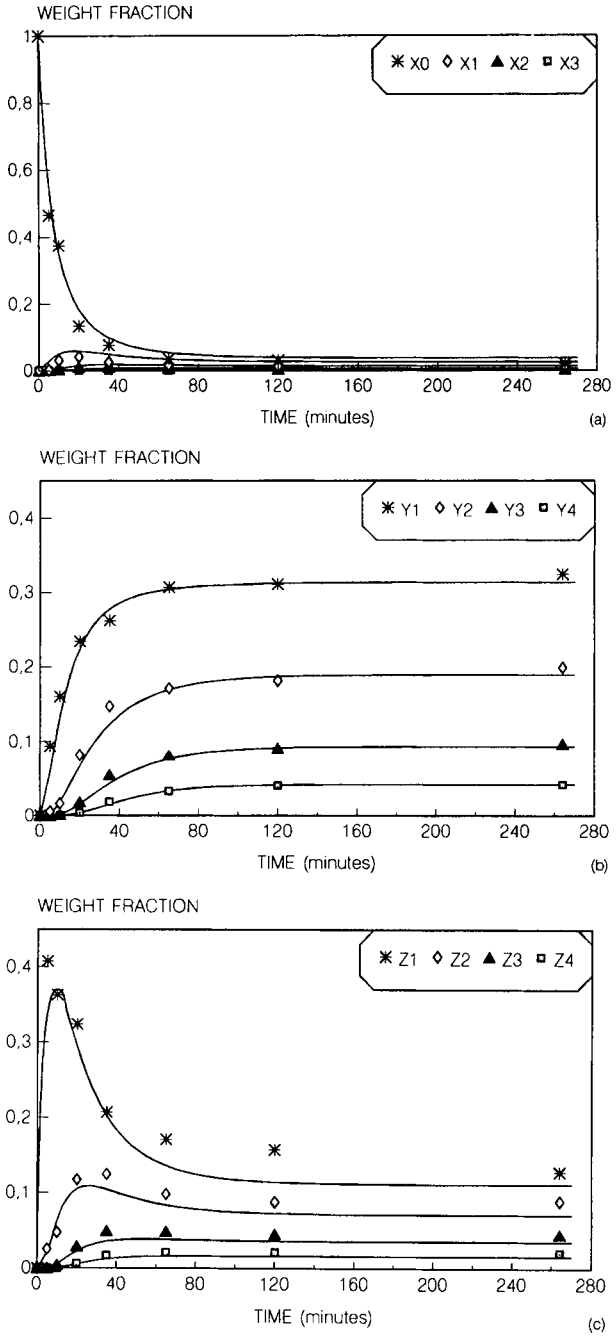

Figure 7 Example of the agreement obtained between experimental and calculated oligomer distributions of the type X (a), Y (b), and Z (c), respectively, related to the run 6.

reported for comparison purposes. A confirmation of the selective behavior of zinc acetate at the lowest concentrations can be appreciated from the data reported in this figure.

In Table VIII, a comparison is reported between a calculation made on run 6 of Table IV, taking account of 4 and 5 reaction sequences, respectively.

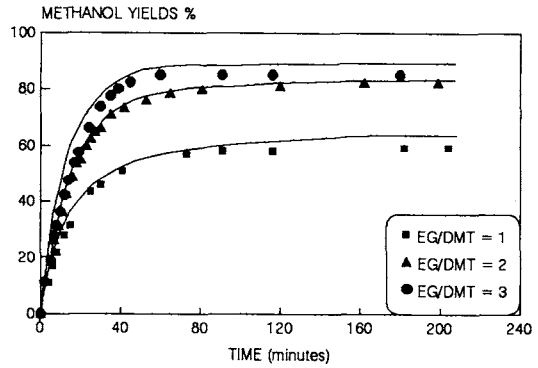

Figure 8 Methanol yields at different times for runs performed at different EG/DMT ratios (runs 6, 11, and 12). Symbols are experimental data, lines are calculated.

As it can be seen, the truncation at the fourth reaction sequence is well justified, considering the very small differences in the results obtained with the two calculations compared. However, as melt transesterification is industrially carried out at temperatures higher than those used in our experiments, oligomers distributions are broader in those conditions and the kinetic model considering five sequences becomes necessary.

Discussion on the Reaction Mechanism

Two controversial mechanisms, a coordinative and a ionic one, are reported in literature[13,15–17] to explain the behavior of the melt transesterification reaction of DMT with EG. In both cases, divalent ions act as Lewis acid coordinating the carbonyl group of the ester and activating it to the nucleophilic attack by the oxygen of glycol or the negatively charged oxygen of an alkoxide ion, respectively. In the first case we would have[15]

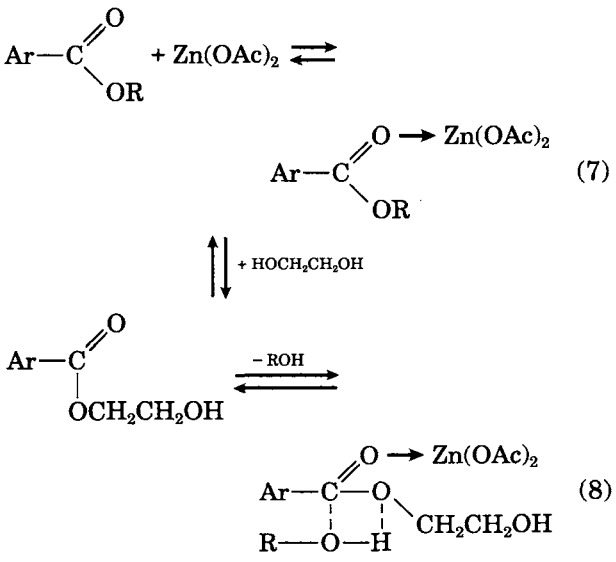

(7)

(8)

where Ar = $RO_2C\ C_6H_4$— and R = CH_3, $HOCH_2CH_2$—

It was even suggested that the metal ion reacts with ethylene glycol to form an alkoxide.[13] Then,

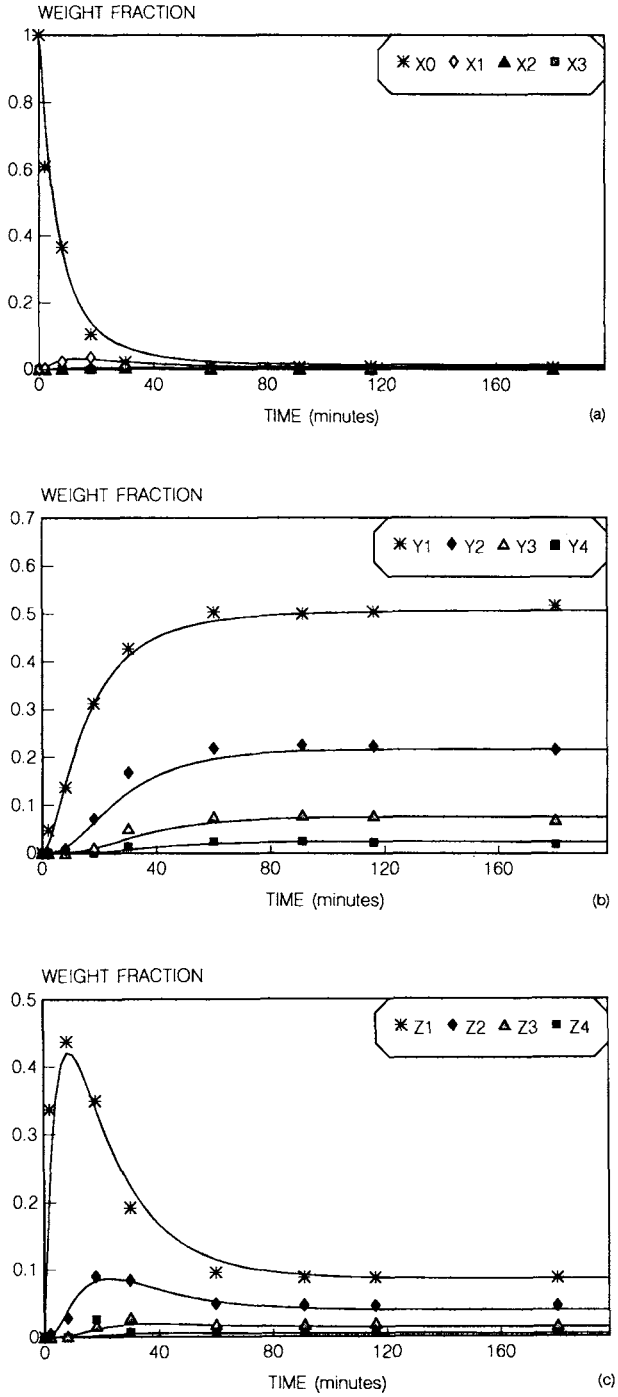

Figure 9 Example of the agreement obtained between experimental and calculated oligomer distributions of the type X (a), Y (b), and Z (c), respectively, related to the run 11.

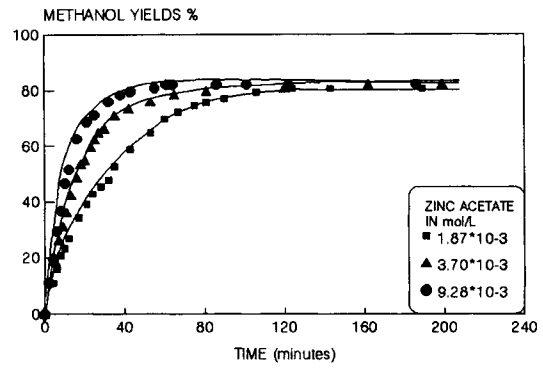

Figure 10 Methanol yields at different times for runs performed at different catalyst concentrations (runs 4, 6, and 7). Symbols are experimental data, lines are calculated.

alkoxide can be involved in coordinative[16,17] or ionic mechanisms.[17]

The coordinative mechanism is quite similar to that already seen if Zn $(OCH_2CH_2OH)_2$ is considered instead of Zn $(OAc)_2$. For the ionic mechanism we can write:

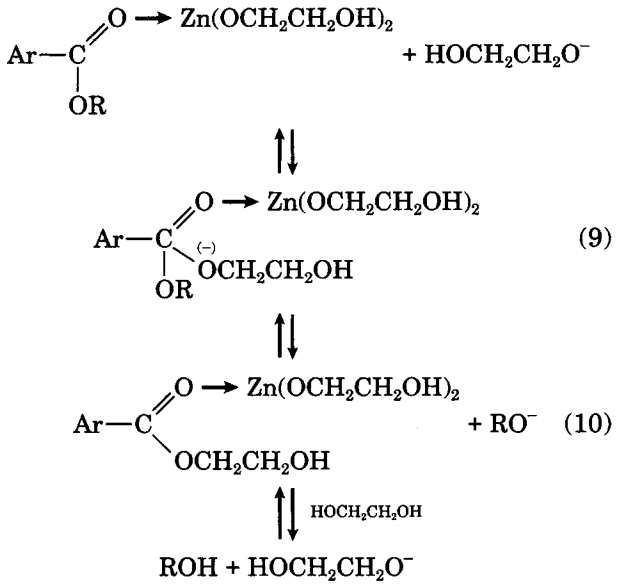

This mechanism is consistent with the reaction orders observed by some authors,[2,13,16,17] that is, first order with respect to ester, glycol, and catalyst. The same kinetics would also be consistent with the coordinative mechanism if the three reagents are assembled together in the same complex.[13,16,17]

However, we observed that the reaction order for the catalyst is about zero for a large concentration range and the first order could be assumed only for very low catalyst concentrations and for the reactions of esters with ethylene glycol, as shown in Figure 5. The reactions of the esters with chain terminal hydroxyls, on the contrary, can be considered of zero order in all the examined concentration fields.

Other authors,[1-3,6,7] too, observed no linear correlation between activity and catalyst concentration except at low catalyst concentrations. Besnoin et al.[1] attributed this behavior to the dissociation equilibrium of zinc acetate:

$$Zn(OAc)_2 \leftrightarrow Zn^{2+} + 2OAc^- \qquad (11a)$$

and Zn^{2+} should be the actual catalyst, through a mechanism similar to that already reported,[7,8] and where Zn^{2+} is considered instead of $Zn(OAc)_2$. We agree with the observation that dissociation is responsible for the change of activity with the catalyst concentration, but we think that not only Zn^{2+} can activate the carbonyl group of the ester, but even an ionic couple containing zinc. Moreover, if the ionic couple contains alkoxides, the ionic mechanism seems to be more reliable because the nucleophylic attack to the carbon atom of the activated carbonyl group is more probable. To conclude, we propose two different activity levels for the undissociated and dissociated ionic couple, respectively, where the metal plays the role of activating the carbonyl group of the ester and alkoxide anions provides a nucleophylic attack to the corresponding carbon atom. Therefore, according to Guibe and Brown[18] for the overall kinetic constant k_1 we can write

$$k_1 = \alpha k_i + (1 - \alpha) k_p$$

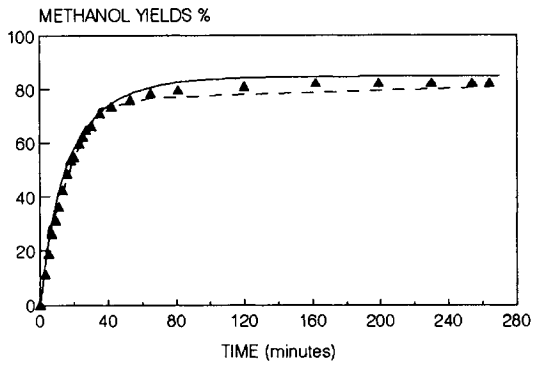

Figure 11 Methanol yields, respectively, from direct measurement and from mass balance (hatching line). Symbols are experimental data, lines are calculated.

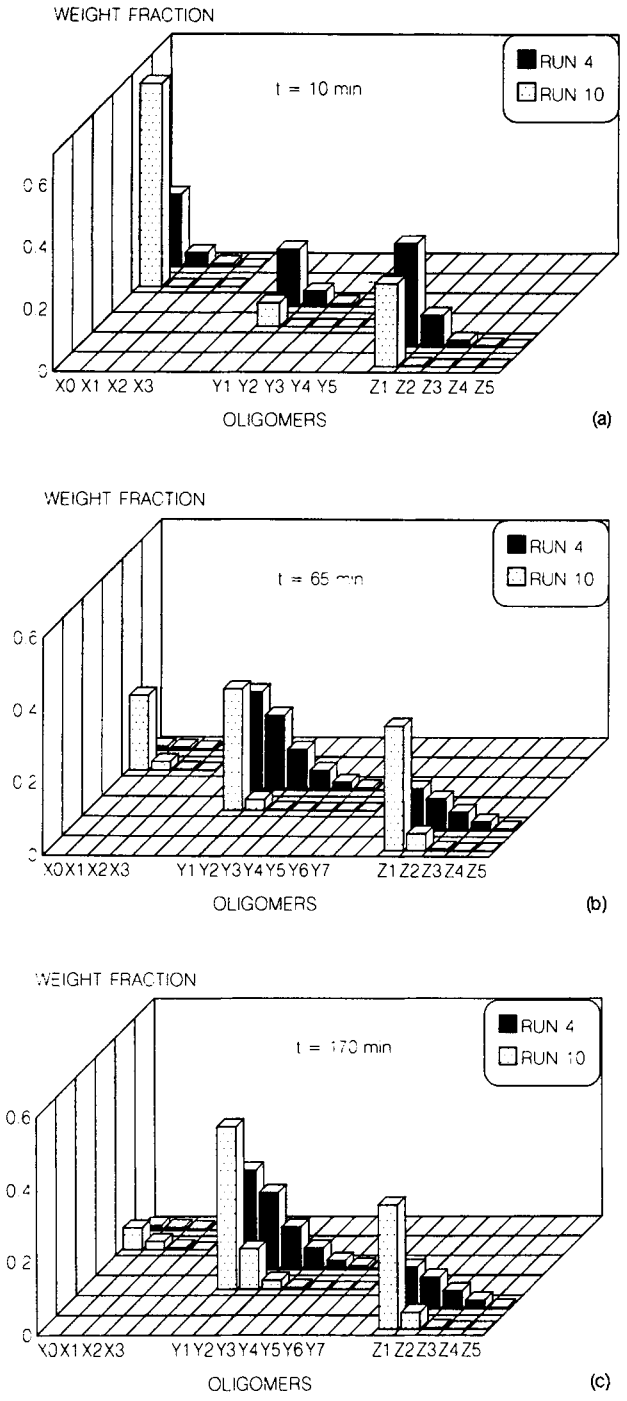

Figure 12 Comparison between the oligomers distributions obtained in two different runs (4 and 10) performed at the lowest and highest catalyst concentration, respectively, at three different reaction times, (a) = 10 min, (b) = 65 min, (c) = 170 min.

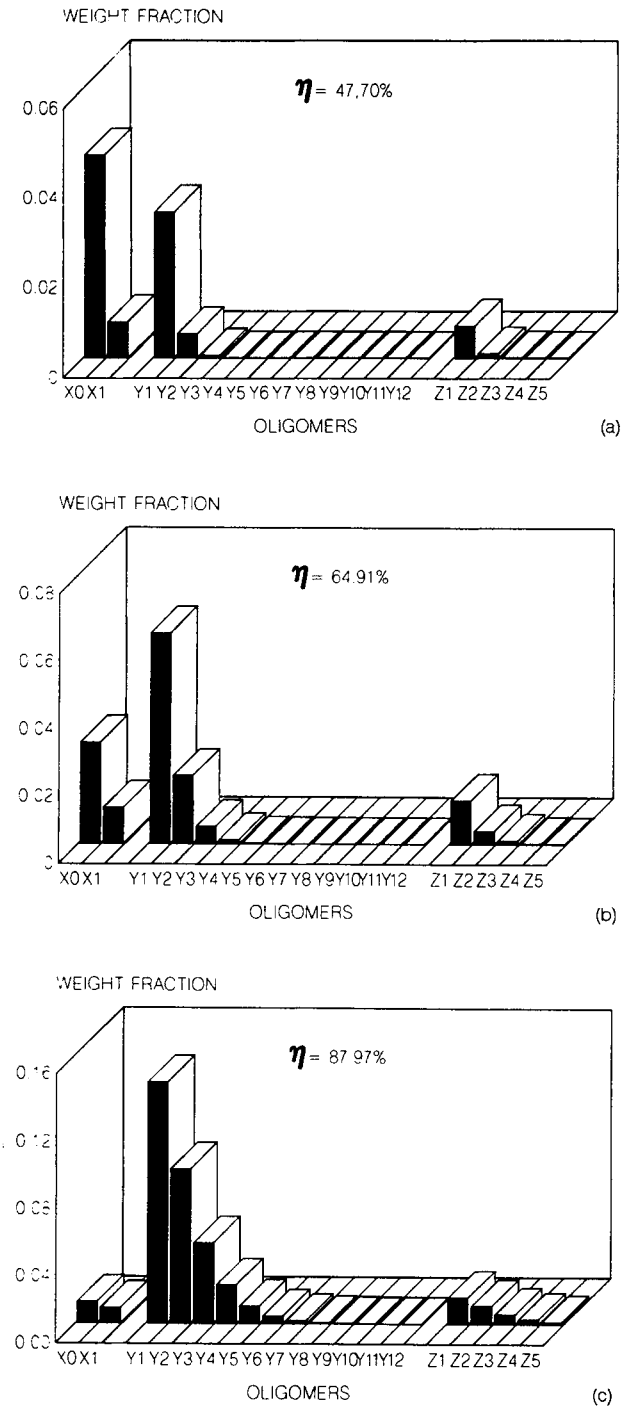

Figure 13 Evolution of the oligomers distributions for different methanol yields obtained by extrapolating the use of the kinetic model at 200°C.

Table VIII Difference in the Oligomers Concentrations Obtained When Considering Four or Five Sequences in the Reaction Scheme

Oligomers X_i	4 Stage wt/wt tot	5 Stage wt/wt tot	Oligomers Y_i	4 Stage wt/wt tot	5 Stage wt/wt tot	Oligomers Z_i	4 Stage wt/wt tot	5 Stage wt/wt tot
X_0(DMT)	5,254E-02	5,248E-02	Y_0 (EG)	1,913E-01	1,913E-01	Z_1 (MHET)	1,284E-01	1,282E-01
X_1	3,381E-02	3,374E-02	Y_1 (BHET)	3,080E-01	3,078E-01	Z_2	7,715E-02	7,695E-02
X_2	1,637E-02	1,632E-02	Y_2	1,749E-01	1,746E-01	Z_3	3,645E-02	3,634E-02
X_3	7,052E-03	7,026E-03	Y_3	8,086E-02	8,072E-02	Z_4	1,550E-02	1,545E-02
X_4	2,851E-03	2,836E-03	Y_4	3,403E-02	3,393E-02	Z_5	6,218E-03	6,190E-03
X_5	1,105E-03	1,098E-03	Y_5	1,355E-02	1,350E-02	Z_6	2,398E-03	2,387E-03
X_6	4,156E-04	4,142E-04	Y_6	5,182E-03	5,181E-03	Z_7	9,008E-04	8,964E-04
X_7	1,455E-04	1,529E-04	Y_7	1,827E-03	1,938E-03	Z_8	3,128E-04	3,300E-04
X_8	0E + 00	5,558E-05	Y_8	0E + 00	7,119E-04	Z_9	0E + 00	1,197E-04
X_9	0E + 00	1,995E-05	Y_9	0E + 00	2,575E-04	Z_{10}	0E + 00	4,289E-05
X_{10}	0E + 00	7,089E-06	Y_{10}	0E + 00	9,217E-05	Z_{11}	0E + 00	1,522E-05
X_{11}	0E + 00	2,498E-06	Y_{11}	0E + 00	3,266E-05	Z_{12}	0E + 00	5,358E-06
X_{12}	0E + 00	8,741E-07	Y_{12}	0E + 00	1,148E-05	Z_{13}	0E + 00	1.873E-06
X_{13}	0E + 00	3,037E-07	Y_{13}	0E + 00	4,004E-06	Z_{14}	0E + 00	6,511E-07
X_{14}	0E + 00	1,042E-07	Y_{14}	0E + 00	1,378E-06	Z_{15}	0E + 00	2,247E-07
X_{15}	0E + 00	3,311E-08	Y_{15}	0E + 00	4,378E-07	Z_{16}	0E + 00	7,072E-08

corresponding to the following reaction scheme:

$$\begin{array}{ccc} Nu^-M^+ & \Leftrightarrow & Nu^- + M^+ \\ \downarrow k_p & & \downarrow k_i \\ \text{Products} & & \text{Products} \end{array} \qquad (11b)$$

where Nu is the nucleophylic group, M is the metal, and α the dissociation degree; so,

$$\alpha = \frac{C_{Nū}}{C_{Nū} - C_{NūM^+}} = \frac{C_{M^+}}{C_{M^+} + C_{NūM^+}} \qquad (12)$$

At low concentrations, $\alpha \rightarrow 1$ and $k_1 \rightarrow k_i$ corresponding to the highest activities; at higher concentrations $\alpha \rightarrow 0$ and, hence, $k_1 \rightarrow k_p$. Considering that zinc is bivalent, a buffer effect would intervene that could justify the reaction order about zero observed for high catalyst concentrations. We have not tried to quantitatively describe the phenomenon because a significant contribution of the coordinative mechanism cannot be excluded and discrimination is not possible with the data available to now.

CONCLUDING REMARKS

We have shown that the possibility of determining the evolution with time of all the oligomeric species in the melt transesterification of DMT with EG allows a more complete kinetic approach to all the reactions occurring. The kinetic model developed in this article could usefully be applied to (1) screen the more suitable catalyst; (2) give evidence of synergic effects when two or more catalysts are employed; (3) model transesterification plants, and (4) give the initial conditions of the prepolymerization step.

Figure 13 shows a simulation of the oligomer distributions for a melt transesterification performed at 200°C in correspondence of different methanol yields. As it can be seen, the final conditions contain only 20% by weight of BHET, together with great amounts of other oligomers of the same type, that is, with two hydroxyls as terminal groups and a unnegligible amount of Z and X type oligomers.

From this figure, it clearly appears that assuming pure BHET as starting prepolymerization reagent, as done in the past, is a not acceptable approximation.

Thanks are due to Montefibre SpA for the financial support.

LIST OF SYMBOLS

$[CH_3OH]$ = Methanol concentration (mol/L).
C_i = Concentration of i component (mol/L).
k_1 = Kinetic constant of transesterification reactions involving EG (L/mol min).

k_2 = Kinetic constant of transesterification reactions not involving EG (L/mol min).
K_{eq1} = Equilibrium constant of transesterification reactions involving EG.
K_{eq2} = Equilibrium constant of transesterification reactions not involving EG.
n_i^0 = Initial mol of i component.
n_i = Number of mol of i component.
r_i = Rate of i formation or disappearing (mol/min).
r_j = Vector of the possible reactions.
$[X_i]$ = Concentration of the X_i species with $i = 0,n$.
X_M = Molar fraction of methanol in the reaction mixture.
R = Constant of gases (cal/mol K).
Y_M = Molar fraction of methanol in the vapor phase.
T = Absolute temperature (K).
P = Pressure (atm).
P^0 = Vapor pressure (atm).
$[Y_i]$ = Concentration of the Y_i species with $i = 0,n$.
$[Z_i]$ = Concentration of the Z_i species with $i = 1,n$.

Greek Symbols

α = Dissociation degree of a generic ionic couple.
α_{ij} = Stoichiometric matrix.
β = Vector of kinetic parameters.
η,η_c, η_s = Methanol yield, subscript c = calculated, s = experimental value.
Φ = objective function.

REFERENCES

1. J. M. Besnoin, G. D. Lei, and K. Y. Choi, *AIChE J.*, **35**(9), 1445 (1989).
2. K. Tomita and H. Ida, *Polymer*, **14**, 55 (1973).
3. T. H. Shah, J. I. Bhatty, G. A. Gamlen, and D. Dollimore, *J. Macromol. Sci.-Chem.*, **A21**(4), 431 (1984).
4. K. Ravindranath, R. A. Mashelkar, *Chem. Eng. Sci.*, **41**(9), 2197 (1986).
5. K. Tomita and H. Ida, *Polymer*, **16**, 185 (1975).
6. G. D. Lei, K. Y. Choi, *Ind. Eng. Chem. Res.*, **31**, 769 (1992).
7. M. J. Barandiaran and J. M. Asua, *Polymer*, **31**, 1347 (1990).
8. G. D. Lei and K. Y. Choi, *Ind. Eng. Chem. Res.*, **32**, 800 (1993).
9. L. M. Zaborsky, II, *Anal. Chem.*, **49**(8), 1166 (1977).
10. G. Buzzi-Ferraris, *Analisi e Identificatione dei Modelli.* CLUP, Milano, Italy, 1975.
11. J. Yamanis and M. Adelman, *J. Polym. Sci.*, **14**, 1961 (1976).
12. S. G. Hovenkamp, *J. Polym. Sci. A-1*, **9**, 3617 (1971).
13. C. M. Fontana, *J. Polym. Sci. A-1*, **6**, 2343 (1968).
14. K. Ravindranath and R. A. Mashelkar, *J. Polym. Sci.: Polym. Chem. Ed.*, **20**, 3447 (1982).
15. K. H. Wolf, B. Kuster, H. Herlinger, C. J. Tschang, and E. Scrhollmeyer, *Angew. Makromol. Chem.*, **68**, 23 (1978).
16. K. Yoda, K. Kimoto, and T. Toda, *J. Chem. Soc. Jpn., Ind. Chem. Sect.*, **67**, 909 (1964).
17. J. Otton, S. Ratton, V. A. Vasnev, G. D. Markova, K. M. Nametov, V. I. Bakhmutov, L. I. Komarova, S. V. Vinogradova, and V. V. Korshak, *J. Polym. Sci., Part A*, **26**(8), 2199 (1988).
18. F. Guibe and G. Bram, *Bull. Soc. Chim. Fr.*, **3–4**, 933 (1975).

Received March 17, 1994
Accepted June 1, 1994